A Three-Photon Probe with Dual Emission Colors for Imaging of Zn(II) Ion in Living Cells

ARTICLE *in* CHEMICAL COMMUNICATIONS · SEPTEMBER 2014

Impact Factor: 6.83 · DOI: 10.1039/C4CC05999A

5 AUTHORS, INCLUDING:

Amal kumar Mandal
University of Twente
34 PUBLICATIONS **482** CITATIONS
SEE PROFILE

Tingchao He
Nanyang Technological University
47 PUBLICATIONS **583** CITATIONS
SEE PROFILE

Handong Sun
Nanyang Technological University
250 PUBLICATIONS **3,494** CITATIONS
SEE PROFILE

ChemComm

COMMUNICATION

View Article Online
View Journal | View Issue

Cite this: *Chem. Commun.*, 2014, **50**, 14378

Received 1st August 2014,
Accepted 29th September 2014

DOI: 10.1039/c4cc05999a

www.rsc.org/chemcomm

A three-photon probe with dual emission colors for imaging of Zn(II) ions in living cells†

Amal Kumar Mandal,‡[a] Tingchao He,‡[bc] Swarup Kumar Maji,[a] Handong Sun*[c] and Yanli Zhao*[ad]

A novel three-photon probe for the imaging of exogenous Zn(II) ions in live cells with varying emission colors under three-photon excitation is developed. The tuning of the charge transfer state and the emission color of the probe was also demonstrated in the presence of acid.

In order to address the issue that the spatial resolution decreases rapidly as a function of the imaging depth,[1] in the last few years a two-photon excitation (2PE) process has been employed to significantly extend the penetration depth in optical imaging.[2] However, the main limitation of the 2PE process in imaging is the poor signal-to-background ratio due to the heterogeneous nature of tissues that scatter strongly.[3] An effective strategy to overcome this shortcoming on imaging is the use of a longer excitation wavelength along with a three-photon excitation (3PE) process. The main advantage of the 3PE process is its significant improvement in the overall excitation localization as a result of the improved signal-to-background ratio by orders of magnitude when compared to the 2PE process.[4] Despite this advantage, a major limitation of the 3PE process is the lack of water-soluble probes with a high three-photon cross-section and brightness for the detection of biologically important metal ions. Among the metal ions, zinc is the second most abundant metal ion in human body, which is present in over 300 metalloproteins as a structural or catalytic component responsible for various biological functions such as DNA repair, regulation of the caspase activity and apoptosis, and modulation of neurotransmission.[5] Pathological disruptions in zinc homeostasis lead to some diseases including brain trauma and seizure, depression, diabetes, prostate cancer and neurodegenerative diseases like Alzheimer's disease.[6] Thus, tremendous efforts have been made for developing new methods and techniques to realize real-time detection and noninvasive imaging of physiological zinc ions.[7]

Among several design strategies reported in the literature for selective detection of zinc ions, the centrosymmetric molecules with the donor–π–acceptor–π–donor (D–π–A–π–D) architecture generally exhibit large cross-section values.[8] Due to a highly polarized excited state, however, they show enhanced solvent–solute interaction in water, which promotes the non-radiative deactivation, and as a result, drastically reduces the brightness.[9] Conversely, the main limitation imposed by turn-on probes[10] for increasing the brightness on imaging is the use of single detection window and/or a short excitation wavelength. In contrast, a probe with a dual emission response provides practical advantages such as built-in corrections for such variability by allowing simultaneous detection of two signals resulting from the two states of the probe.[11]

In this context, we designed a simple D–π–A system (L1 in Fig. 1), which consists of aniline and pyrrole units as two

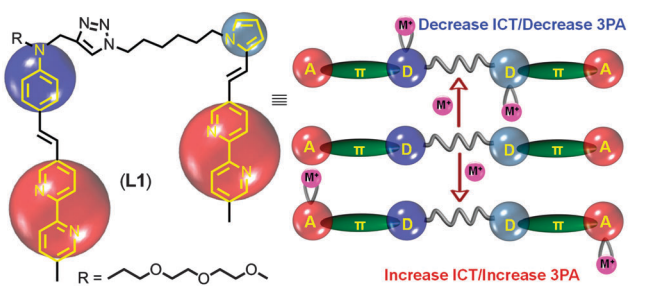

Fig. 1 Chemical structure of probe (L1) and the schematic representation for the modulation of the three-photon absorption (3PA) response of the probe upon binding with M^{n+} (Mn^{+} = Zn^{2+} and H^{+}).

[a] *Division of Chemistry and Biological Chemistry, School of Physical and Mathematical Sciences, Nanyang Technological University, 21 Nanyang Link, 637371, Singapore. E-mail: zhaoyanli@ntu.edu.sg*
[b] *College of Physics Science and Technology, Shenzhen University, Shenzhen 518060, China*
[c] *Division of Physics and Applied Physics, Centre for Disruptive Photonic Technologies (CDPT), School of Physical and Mathematical Sciences, Nanyang Technological University, 21 Nanyang Link, 637371, Singapore. E-mail: hdsun@ntu.edu.sg*
[d] *School of Materials Science and Engineering, Nanyang Technological University, 50 Nanyang Avenue, 639798, Singapore*

† Electronic supplementary information (ESI) available: Additional synthesis and characterization details. See DOI: 10.1039/c4cc05999a

‡ These authors contributed equally to this work.

different donors respectively connected with 2,2′-bipyridine as a common acceptor through π-conjugation. The two units were bridged by a triazole moiety formed through click chemistry. The 2,2′-bipyridine moiety was chosen as the acceptor on account of its strong electron-deficient nature and ability to bind with Zn(II) ions. The introduction of the aniline moiety is to provide the substitution of the N-atom with a water-compatible glycol side chain in order to increase the water solubility of the probe. Such a structural design not only increases the three-photon cross-section and brightness with enhanced transition dipole moment in the presence of Zn(II) ions in water, but also facilitates tuning of the charge transfer band of the probe with varied emission colors in the presence of trifluoroacetic acid (TFA).

The synthetic procedure for probe L1 is shown in the ESI† (Fig. S1). Solvatochromic behavior of probe L1, exhibited from steady-state fluorescence response, shows a 60 nm bathochromic shift of the emission maximum with a visual color change from blue to green upon increasing the solvent polarity (ESI,† Fig. S2). Among different metal perchlorate salts, an obvious red shift of the absorption maximum was observed only in the case of Zn(II) ions (ESI,† Fig. S3 and S4). Systematic titration revealed that the band at 380 nm decreased with concomitant appearance of a new red-shifted band ($\Delta\lambda$ = 46 nm) at 426 nm (Fig. 2a). Good linear fit of the Benesi–Hildebrand plot (B–H plot) suggests the 1 : 2 binding stoichiometry and the formation of complex L1[Zn^{2+}]$_2$ with the association constant $K_{L1[Zn^{2+}]2}^{A}$ = 1.19 × 10^{10} M^{-2} L^{-2} (ESI,† Fig. S8).[12] The 1 : 2 binding stoichiometry between L1 and Zn(II) was also evaluated from the molar ratio plot (ESI,† Fig. S12) and the high-resolution mass spectrum (ESI,† Fig. S13). The fluorescence spectrum of L1 showed an intense band (Φ = 0.27) with an emission maximum at 515 nm under excitation at 380 nm.

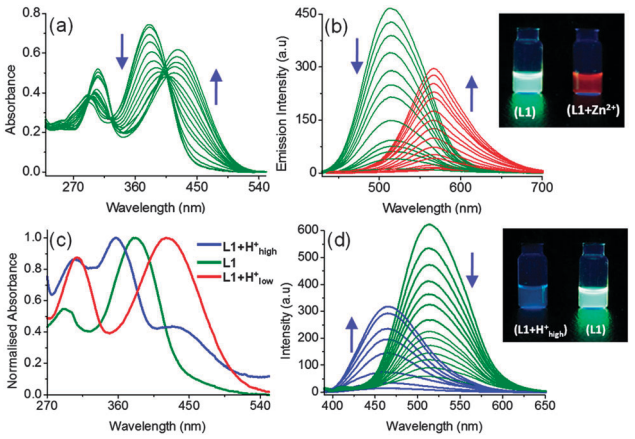

Fig. 2 Changes in (a) UV-vis spectra of L1 (1.18 × 10^{-5} M) upon increasing the concentration of Zn(II) (0–1.77 × 10^{-4} M). (b) Fluorescence spectra of L1 (5.98 × 10^{-6} M) upon increasing the concentration of Zn(II) (0–1.31 × 10^{-4} M) under excitation at 380 nm recorded in 50 mM aqueous HEPES buffer (pH 7.2) at 25 °C. (c) Normalized UV-vis spectral changes of L1 (1.05 × 10^{-5} M) in the presence of low (1.60 × 10^{-3} M, H_{low}^{+}) and high (5.00 × 10^{-2} M, H_{high}^{+}) concentrations of TFA. (d) Fluorescence spectral changes of L1 (1.05 × 10^{-5}) with varying concentrations of TFA (0–5.00 × 10^{-2} M) under excitation at 380 nm recorded in water (0.1 M KCl) at 25 °C. The inset figure indicates the visual color change of L1 in the presence of Zn^{2+} and TFA.

During the initial addition of Zn(II) (0–4 equiv.), the emission band at 515 nm exhibited a decrease of the emission intensity (Fig. 2b, green curve). A new red-shifted band ($\Delta\lambda$ = 51 nm, Fig. 2b, red curve) at 566 nm appeared with increasing emission intensity (Φ = 0.18) upon further additions of Zn(II) (5–22 equiv.). Two distinct fluorescence changes enabled us to evaluate the stepwise binding constants for the complexation of L1 with Zn(II). The respective binding constants for the formations were calculated, $K_{L1[Zn^{2+}]}^{1}$ = 1.54 × 10^{7} M^{-1} L and $K_{L1[Zn^{2+}]2}^{2}$ = 1.73 × 10^{3} M^{-1} L (ESI,† Fig. S9 and S10). The nice fit of the titration profile of the fluorescence response revealed a good selectivity of the probe towards Zn(II) with a large dynamic range from 5.98 × 10^{-8} M to 1.01 × 10^{-5} M and a low detection limit of 0.13 mg L^{-1} or 0.13 ppm (ESI,† Fig. S7a). The reversible binding nature of probe L1 towards Zn(II) was demonstrated in the presence of ethylenediaminetetraacetic acid (EDTA) by monitoring the fluorescence spectral change (ESI,† Fig. S19).

Upon initial additions of TFA (0–1.6 × 10^{-3} M, H_{low}^{+}), the absorption maximum of probe L1 at 380 nm decreased with simultaneous increases of a red-shifted band at 425 nm (ESI,† Fig. S6a and b). However, the corresponding emission maximum at 515 nm decreased with 52% drop in the emission quantum yield (Φ = 0.14). A blue-shifted absorption maximum at 355 nm appeared upon further addition of TFA (1.8 × 10^{-3}–5.0 × 10^{-2} M, H_{high}^{+}) to this solution (ESI,† Fig. S6c and d), and a new blue-shifted emission peak (Fig. 2c) emerged at 465 nm with an increase in the quantum yield (Φ = 0.26). The possible binding mechanism and geometry are shown in Fig. S11 (ESI†). Time resolved fluorescence experiments also suggested the complexation of probe L1 with Zn(II) and its tunable charge transfer nature in the presence of TFA (ESI,† Table S1 and Fig. S14). In addition, the sequential protonation process and the binding geometry of probe L1 with Zn(II) were established through ^{1}H NMR titration (ESI,† Fig. S15 and S16).

We next investigated the three-photon luminescence (3PL) characteristics of L1 in the absence and presence of Zn(II) or TFA under excitation in the NIR region. When excited at 1200 nm, L1 showed an intense emission band with the maximum at 518 nm (Fig. 3a). The logarithmic plot of photoluminescence intensity as a function of incident laser power with a slope of ~3 further confirmed the three-photon emission process (Fig. 3b and ESI,† Fig. S17). Upon increasing the concentration of Zn(II), the 3PL intensity at 515 nm initially decreased and a new red-shifted band with the maximum at 591 nm emerged (Fig. 3a and ESI,† Fig. S18). Upon the initial addition of TFA (9.1 × 10^{-4} M, H_{low}^{+}), the 3PL intensity at 515 nm decreased (Fig. 3a). A blue-shifted band at 466 nm with increasing emission intensity emerged upon further addition of TFA (2.8 × 10^{-2} M, H_{high}^{+}). The normalized 3PL response of probe L1 with a tunable emission color in the presence of Zn(II) or H^{+} is shown in Fig. 3d. The 3PA cross-sections of the samples were determined by the multiphoton excited luminescence method using Rhodamine B as the reference (ESI,† page S22). Fig. 3c exhibits 3PA spectra of probe L1 in the presence of Zn(II) or TFA, and the corresponding data are summarized in Table S2 (ESI†). When monitoring at 1200 nm, probe L1 gave a 3PA

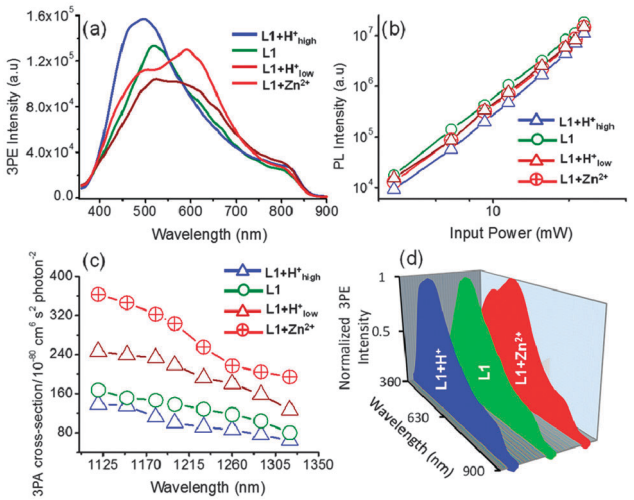

Fig. 3 (a) Three-photon excited emission spectra of L1 (5.98×10^{-6} M) in the presence of Zn^{2+} (1.31×10^{-4} M) or TFA (9.10×10^{-4} M, H_{low}^{+}; 2.84×10^{-2} M, H_{high}^{+}) under excitation at 1200 nm. (b) The corresponding logarithmic plots of the luminescence output *vs.* incident power intensity. (c) 3PA spectra of L1 (5.98×10^{-6} M) in the presence of Zn^{2+} (1.31×10^{-4} M) or TFA (9.10×10^{-4} M, H_{low}^{+}; 2.84×10^{-2} M, H_{high}^{+}). (d) The normalized three-photon excited emission spectral response of L1 in the presence of Zn^{2+} (1.31×10^{-4} M) or TFA (H_{high}^{+}, 2.84×10^{-2} M), showing the tunability of the emission color from blue to red. In the case of Zn^{2+}, the spectra were recorded in 50 mM aqueous HEPES buffer (pH 7.2) at 25 °C, whereas the spectra were recorded in water (0.1 M KCl) at 25 °C in the case of TFA.

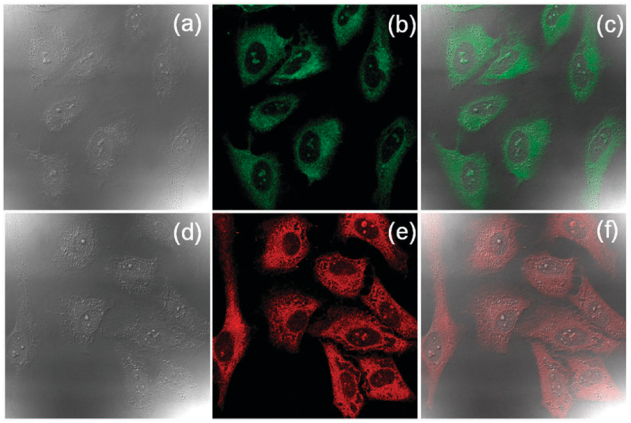

Fig. 4 Three-photon microscopy images of HeLa cells under excitation at 1200 nm. (a) The bright field image of live HeLa cells stained with 10 μM probe L1 for 4 h. (b) The corresponding dark field image of Hela cells, and the emission was collected at 500–600 nm. (c) The overlay image of (a) and (b). (d) The bright field image of live HeLa cells stained with 10 μM probe L1 for 4 h followed by treating with 90 μM $ZnCl_2$ for 2 h. (e) The corresponding dark field image, and the emission was collected at 600–700 nm. (f) The overlay image of (d) and (e).

cross-section (σ_3) of 1.38×10^{-78} cm^6 s^2 photon^{-2}. The value is four orders of magnitude higher than those of some previously reported organic dyes[2b,4b,13] and one order of magnitude higher than that of the recently reported ZnS:Mn nanocrystal.[14] Interestingly, about three times increase in the cross-section value ($\sigma_3 = 3.03 \times 10^{-78}$ cm^6 s^2 photon^{-2}) was observed after coordination with Zn(II) (Fig. 3c). The increase in the transition dipole moment between the ground and final states upon coordination with Zn(II) was responsible for increasing the cross-section value.[15] The 3PA spectra and the cross-section values of L1 in the presence of TFA once again supported the conclusion (Fig. 3c and ESI,† Table S2). The initial protonation of the 2,2′-bipyridine moieties increases the cross-section value ($\sigma_3 = 2.18 \times 10^{-78}$ cm^6 s^2 photon^{-2}). Further protonation of the amine moiety decreased the transition dipole moment as well as the 3PA cross-section value ($\sigma_3 = 1.00 \times 10^{-78}$ cm^6 s^2 photon^{-2}).

Probe L1 consists of two different binding sites for protonation, *i.e.*, the 2,2′-bipyridine unit (acceptor moiety) and the aniline unit (donor moiety). Thus, it is possible to tune the intramolecular charge transfer (ICT) nature of the probe in the presence of acid, which was demonstrated by the above mentioned optical response of the probe in the presence of TFA. At a low concentration of H^+, which favors the protonation of the 2,2′-bipyridine unit, the ICT nature of the probe was increased, and as a result, a red shift in the UV-vis spectra was observed (Fig. 2c). At a high concentration of H^+, which favors the protonation of the aniline unit, the ICT nature of the probe was increased, and a blue shift in the UV-vis spectra was detected (Fig. 2c). The tunability of the ICT state of the probe was also established through the change in the 3PA cross-section value in the presence of acid. Since the initial protonation of the 2,2′-bipyridine unit increased the ICT nature as well as the transition dipole moment of the probe, an increased cross-section value was observed. Upon further protonation of the aniline unit, the transition dipole moment and the 3PA cross-section value decreased (ESI,† Fig. S11). Thus, the tunability of the ICT nature of the probe by changing the charge transfer band in the presence of TFA was well verified through the detailed spectroscopic measurements. The probe exhibits not only acid-induced ICT tunability, but also Zn(II)-sensing capability.

3-(4,5-Dimethylthiazol-2-yl)-2,5-diphenyltetrazolium bromide (MTT) assay revealed that the cellular viabilities of HeLa cells were greater than 80% after incubation with 110 μM probe for 24 h (ESI,† Fig. S20), indicating low cytotoxicity of the probe. This observation encouraged us to detect the presence of exogenous Zn(II) ions in live cells using the probe (Fig. 4). Upon three-photon excitation at 1200 nm, the fluorescence image of HeLa cells endocytosed with 10 μM probe L1 showed dark green fluorescence (Fig. 4b). Interestingly, dark red fluorescence images were observed when the cells were stained with 10 μM probe L1 followed by incubation with 90 μM $ZnCl_2$ (Fig. 4e). These experiments demonstrated that probe L1 could be able to detect the presence of exogenous Zn(II) ions in live HeLa cells, with the emission color change from green to red under three-photon excitation at 1200 nm.

In conclusion, we have demonstrated the synthesis and application of a novel three-photon probe for the detection of Zn(II) ions in water and *in vitro*. The appropriate design of the probe with a donor–acceptor architecture facilitates tuning of its 3PA cross-section as well as the emission color. The low cytotoxicity and good cell-permeability of the probe are beneficial to visualize the presence of exogenous Zn(II) ions in live HeLa cells with a distinct emission color change from green to red under three-photon

excitation. Thus, this three-photon probe may find its way into real-time detection of physiological Zn(II) ions in the future.

This research was supported by the National Research Foundation (NRF), Prime Minister's Office, Singapore under its NRF Fellowship (NRF2009NRF-RF001-015), Campus for Research Excellence and Technological Enterprise (CREATE) Programme–Singapore Peking University Research Centre for a Sustainable Low-Carbon Future, and Competitive Research Programme (CRP) under Project No. NRF-CRP5-2009-04, as well as the NTU-A*Star Centre of Excellence for Silicon Technologies (A*Star SERC No. 112 351 0003).

Notes and references

1 V. Ntziachristos, *Nat. Methods*, 2010, **7**, 603.
2 (*a*) W. Denk, J. Strickler and W. Webb, *Science*, 1990, **248**, 73; (*b*) C. Xu, W. Zipfel, J. B. Shear, R. M. Williams and W. W. Webb, *Proc. Natl. Acad. Sci. U. S. A.*, 1996, **93**, 10763; (*c*) W. R. Zipfel, R. M. Williams and W. W. Webb, *Nat. Biotechnol.*, 2003, **21**, 1369; (*d*) F. Helmchen and W. Denk, *Nat. Methods*, 2005, **2**, 932.
3 D. Kobat, N. G. Horton and C. Xu, *J. Biomed. Opt.*, 2011, **16**, 106014.
4 (*a*) D. Kobat, M. E. Durst, N. Nishimura, A. W. Wong, C. B. Schaffer and C. Xu, *Opt. Express*, 2009, **17**, 13354; (*b*) N. G. Horton, K. Wang, D. Kobat, C. G. Clark, F. W. Wise, C. B. Schaffer and C. Xu, *Nat. Photonics*, 2013, **7**, 205.
5 (*a*) B. L. Vallee and K. H. Falchuk, *Physiol. Rev.*, 1993, **73**, 79; (*b*) C. F. Walker and R. E. Black, *Annu. Rev. Nutr.*, 2004, **24**, 255; (*c*) C. J. Frederickson, *Int. Rev. Neurobiol.*, 1989, **31**, 145; (*d*) E. Ho and B. N. Ames, *Proc. Natl. Acad. Sci. U. S. A.*, 2002, **99**, 16770; (*e*) E. Kimura, S. Aoki, E. Kikuta and T. Koike, *Proc. Natl. Acad. Sci. U. S. A.*, 2003, **100**, 3731.
6 (*a*) D. W. Choi and J. Y. Koh, *Annu. Rev. Neurosci.*, 1998, **21**, 347; (*b*) J. García-Colunga, E. Vázquez-Gómez and R. Miledi, *Pharmacogenomics J.*, 2004, **4**, 388; (*c*) A. B. Chausmer, *J. Am. Coll. Nutr.*, 1998, **17**, 109; (*d*) S. M. Henshall, *Oncogene*, 2003, **22**, 6005; (*e*) M. P. Cuajungco and G. J. Lees, *Neurobiol. Dis.*, 1997, **4**, 137; (*f*) A. I. Bush, *Alzheimer Dis. Assoc. Disord.*, 2003, **17**, 147.
7 (*a*) A. Ajayaghosh, P. Carol and S. Sreejith, *J. Am. Chem. Soc.*, 2005, **127**, 14962; (*b*) S. Sreejith, K. P. Divya and A. Ajayaghosh, *Chem. Commun.*, 2008, 2903; (*c*) K. P. Divya, S. Sreejith, P. Ashokkumar, K. Yuzhan, Q. Peng, S. K. Maji, Y. Tong, H. Yu, Y. Zhao, P. Ramamurthyc and A. Ajayaghosh, *Chem. Sci.*, 2014, **5**, 3469; (*d*) K. P. Divya, S. Sreejith, C. H. Suresh and A. Ajayaghosh, *Chem. Commun.*, 2010, **46**, 8392; (*e*) S. Sreejith, K. P. Divya, T. K. Manojkumar and A. Ajayaghosh, *Chem. – Asian J.*, 2011, **6**, 430; (*f*) S. Sreejith, K. P. Divya, P. Jayamurthy, J. Mathew, V. N. Anupama, D. S. Philips, P. Aneesa and A. Ajayaghosh, *Photochem. Photobiol. Sci.*, 2012, **11**, 1715.
8 (*a*) G. S. He, L.-S. Tan, Q. Zheng and P. N. Prasad, *Chem. Rev.*, 2008, **108**, 1245; (*b*) J.-X. Yang, C.-X. Wang, L. Li, N. Lin, X.-T. Tao, Y.-P. Tian, X. Zhao and M.-H. Jiang, *Chem. Phys.*, 2009, **358**, 39.
9 H. Y. Woo, B. Liu, B. Kohler, D. Korystov, A. Mikhailovsky and G. C. Bazan, *J. Am. Chem. Soc.*, 2005, **127**, 14721.
10 (*a*) H. M. Kim and B. R. Cho, *Acc. Chem. Res.*, 2009, **42**, 863; (*b*) G. Masanta, C. S. Lim, H. J. Kim, J. H. Han, H. M. Kim and B. R. Cho, *J. Am. Chem. Soc.*, 2011, **133**, 5698.
11 (*a*) S. K. Bae, C. H. Heo, D. J. Choi, D. Sen, E.-H. Joe, B. R. Cho and H. M. Kim, *J. Am. Chem. Soc.*, 2013, **135**, 9915; (*b*) H. J. Kim, C. H. Heo and H. M. Kim, *J. Am. Chem. Soc.*, 2013, **135**, 17969; (*c*) S. Sumalekshmy, M. M. Henary, N. Siegel, P. V. Lawson, Y. Wu, K. Schmidt, J.-L. Brédas, J. W. Perry and C. J. Fahrni, *J. Am. Chem. Soc.*, 2007, **129**, 11888.
12 A. K. Mandal, M. Suresh, P. Das, E. Suresh, M. Baidya, S. K. Ghosh and A. Das, *Org. Lett.*, 2012, **14**, 2980.
13 (*a*) S. Maiti, J. B. Shear, R. M. Williams, W. R. Zipfel and W. W. Webb, *Science*, 1997, **275**, 530; (*b*) W. R. Zipfel, R. M. Williams, R. Christie, A. Y. Nikitin, B. T. Hyman and W. W. Webb, *Proc. Natl. Acad. Sci. U. S. A.*, 2003, **100**, 7075.
14 J. H. Yu, S.-H. Kwon, Z. Petrášek, O. K. Park, S. W. Jun, K. Shin, M. Choi, Y. I. Park, K. Park, H. B. Na, N. Lee, D. W. Lee, J. H. Kim, P. Schwille and T. Hyeon, *Nat. Mater.*, 2013, **12**, 359.
15 P. Cronstrand, B. Jansik, D. Jonsson, Y. Luo and H. Ågren, *J. Chem. Phys.*, 2004, **121**, 9239.